Computational Mechanics 27 (2001) 412–417 © Springer-Verlag 2001

Numerical simulation of gas-particle flows behind a backward-facing step using an improved stochastic separated flow model

C. K. Chan, H. Q. Zhang, K. S. Lau

Abstract An improved stochastic separated flow (ISSF) model developed by the present authors is tested in gas-particle flows behind a backward-facing step, in this paper. The gas phase of air and the particle phase of 150 μm glass and 70 μm copper spheres are numerically simulated using the k–ε model and the ISSF model, respectively. The predicted mean streamwise velocities as well as streamwise and transverse fluctuating velocities of both phases agree well with experimental data reported by Fessler. The reattachment length of $7.6H$ matches well with the experimental value of $7.4H$. Distributions of particle number density are also given and found to be in good agreement with the experiment. The sensitivity of the predicted results to the number of calculation particles is studied and the improved model is shown to require much less calculation particles and less computing time for obtaining reasonable results as compared with the traditional stochastic separated flow model. It is concluded that the ISSF model can be used successfully in the prediction of backward-facing step gas-particle flows, which is characterised by having recirculating regions and anisotropic fluctuating velocities.

Introduction

Two-phase flows are commonly found in many engineering and natural processes, such as pulverized-coal combustion, spray combustion and solid transport. Generally, there are two approaches to predict the properties of the dispersed phase. They are the two-fluid model based on the Eulerian approach and the trajectory model based on the Lagrangian approach (Crowe et al., 1996). In the Lagrangian approach, the stochastic separated flow (SSF) model is widely used among the deterministic separated flow (DSF) model and 'particle diffusion velocity' model (Chang and Yang, 1999).

In the SSF model, the key points are the concept of energy containing eddies and their action on the motion of the dispersed phase. It assumes that the local continuous phase turbulent fluctuation has an effect on the particle turbulent dispersion only for points at the beginning of the interaction time on the whole trajectory (Chan et al., 2000). Therefore, the turbulent interaction between two phases is treated as an intermittent process and a large number of computation particles (in the order 10^4) (Chang and Yang, 1999) needs to be introduced into the prediction for a smooth statistical property of the dispersed phase. Noticing that much less computation particles are needed in the DSF model for smooth statistical results (Chang and Wu, 1994) and that interaction of two phases is a continuous process, the present authors (Chan et al., 2000) have developed an improved stochastic separated flow (ISSF) model, in which mean properties including velocity and mean-square fluctuating velocity are transported along its stochastic trajectory. Instead of considering the turbulent interaction between two phases to be a discrete process as in the SSF model, the mean-square fluctuating velocity is defined along the stochastic trajectory by the transport equation in the ISSF model. This ensures that the turbulent interaction between two phases is continuous within the entire trajectory. Similar to the DSF model, the mean properties are also transported along the trajectory in the ISSF model, thus requiring less computation particles. Therefore, the ISSF model is capable of treating the turbulent interaction between two phases as a continuous process without introducing a large number of computation particles into predictions.

This model has been successfully applied to a turbulent two-phase flow of planar mixing layer as well as sudden-expansion particle-laden flows by Chan et al. (2000) and Zhang et al. (2001). Further test for this model is carried out in this paper in a typical engineering case of gas-particle flow behind a backward-facing step, which has a recirculating region. Detailed experimental information of the two phases, especially the anisotropic fluctuating velocity, is available to test the prediction ability of the anisotropic turbulence of the particle phase.

Basic equations

Backward-facing step gas-particle flows

In order to compare with experimental results, the test case is carried out with the same flow parameters and

Received 20 June 2000

C. K. Chan (✉)
Department of Applied Mathematics,
The Hong Kong Polytechnic University,
Hung Hom, Kowloon, Hong Kong
e-mail: ck.chan@polyu.edu.hk

H. Q. Zhang
Department of Engineering Mechanics, Tsinghua University,
Beijing 100084, China

K. S. Lau
Department of Applied Physics, The Hong Kong Polytechnic University, Hung Hom, Kowloon, Hong Kong

This work was partially supported by the Research Committee of The Hong Kong Polytechnic University (Project Account Codes A-PA81 and G-YC18).

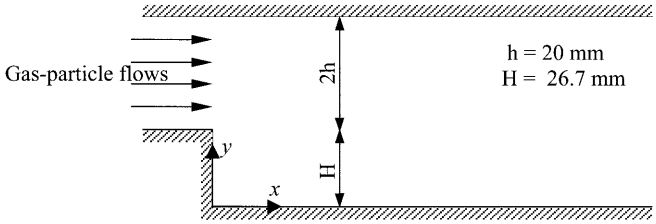

Fig. 1. Test section

geometry of the test section as those of the experiment carried out by Fessler and Eaton (1999). The test section has an expansion ratio of 5:3 as shown in Fig. 1. The flow is a single-sided sudden expansion oriented vertically downward. The Reynolds number of the inlet channel flow, based on the centerline velocity U_0 of 10.5 m/s and the channel half-height, is 13,800; whereas the Reynolds number of the backward facing step, based on the channel centerline velocity and step height is 18,400. 150 μm glass and 70 μm copper spheres are introduced into the backward-facing step flow as the particle phase, their densities are 2500 and 8800 kg/m^3, respectively. The backward-facing step flow is considered to be a steady two-dimensional turbulent gas-particle flow.

Basic equations of gas-phase flow

The k–ε turbulence model is adopted to describe the gas-phase turbulent motion. The general form of Reynolds-averaged equations of continuous phase is given as follows

$$\frac{\partial}{\partial x}(\rho u\varphi)+\frac{\partial}{\partial y}(\rho v\varphi)=\frac{\partial}{\partial x}\left(\Gamma_\varphi\frac{\partial\varphi}{\partial x}\right)+\frac{\partial}{\partial y}\left(\Gamma_\varphi\frac{\partial\varphi}{\partial y}\right)+S_\varphi+S_{p\varphi}\ , \tag{1}$$

where φ is the generalized dependent variable, Γ_φ is the transport coefficient, S_φ is the source term of gas phase of viscosity μ and density ρ, and $S_{p\varphi}$ is the source term due to the gas-particle interaction. The meaning of φ, Γ_φ, S_φ and $S_{p\varphi}$ for each governing equation is given in Table 1. The empirical constants are given in Table 2.

Basic equations of particle-phase flow

The particle phase is simulated in Lagrangian approach using an improved stochastic separated flow model. In the ISSF model, the dispersed phase is treated as individual particles moving through the turbulent flow field of the gas phase, and each of them represents a group of physical particles with the same size, velocity and history. The particle–particle interactions, pressure gradients, virtual mass, Basset and Magnus forces are neglected.

Table 2. Empirical constants

C_μ	C_1	C_2	σ_k	σ_ε
0.09	1.44	1.80	0.8	1.1

The time-averaged velocities u_p^m and v_p^m for the m-th particle in the x-and y-directions are given as

$$\frac{\mathrm{d}u_p^m}{\mathrm{d}t}=u_p^m\frac{\mathrm{d}u_p^m}{\mathrm{d}x_p^m}+v_p^m\frac{\mathrm{d}u_p^m}{\mathrm{d}y_p^m}=\frac{u-u_p^m}{\tau_{rp}^m}\ , \tag{2}$$

and

$$\frac{\mathrm{d}v_p^m}{\mathrm{d}t}=u_p^m\frac{\mathrm{d}v_p^m}{\mathrm{d}x_p^m}+v_p^m\frac{\mathrm{d}v_p^m}{\mathrm{d}y_p^m}=\frac{v-v_p^m}{\tau_{rp}^m}\ , \tag{3}$$

where u and v are the time-averaged velocities of gas phase and τ_{rp}^m is the particle dynamic relaxation time defined by

$$\tau_{rp}^m=\frac{4D_p^m\rho_p^m}{3C_\mathrm{D}^m\rho\sqrt{(u-u_p^m)^2+(v-v_p^m)^2}}\ . \tag{4}$$

The drag coefficient C_D^m for a spherical drop is given by an empirical formula of Putnam (1961),

$$C_\mathrm{D}^m=\frac{24}{\mathrm{Re}_p^m}\left(1+\frac{\mathrm{Re}_p^{m^{2/3}}}{6}\right);\quad \mathrm{Re}_p^m\le 1000\ ,$$
$$=0.44;\quad \mathrm{Re}_p^m>1000\ , \tag{5}$$

where the particle Reynolds number Re_p^m is defined by

$$\mathrm{Re}_p^m=\rho\sqrt{(u-u_p^m)^2+(v-v_p^m)^2}D_p^m/\mu\ , \tag{6}$$

and ρ_p^m and D_p^m are the particle's density and diameter, respectively.

The mean-square fluctuating velocities $\overline{u_p^{m'^2}}$ and $\overline{v_p^{m'^2}}$ for the m-th particle are given as

Table 1. Governing equation of the gas phase

Equation	φ	Γ_φ	S_φ	$S_{p\varphi}$
Continuity	1	0	0	0
Axial momentum	u	μ_e	$-\frac{\partial p}{\partial x}+\frac{\partial}{\partial x}\left(\mu_e\frac{\partial u}{\partial x}\right)+\frac{\partial}{\partial y}\left(\mu_e\frac{\partial v}{\partial x}\right)$	S_{pu}
Transverse momentum	v	μ_e	$-\frac{\partial p}{\partial y}+\frac{\partial}{\partial x}\left(\mu_e\frac{\partial u}{\partial y}\right)+\frac{\partial}{\partial y}\left(\mu_e\frac{\partial v}{\partial y}\right)$	S_{pv}
Turbulent kinetic energy	k	$\frac{\mu_e}{\sigma_k}$	$G_k-\rho\varepsilon$	0
Turbulent kinetic energy dissipation rate	ε	$\frac{\mu_e}{\sigma_\varepsilon}$	$\frac{\varepsilon}{k}(C_1G_k-C_2\rho\varepsilon)$	0

$$\mu_e=\mu+\mu_t,\ \mu_t=C_\mu\rho k^2/\varepsilon,\ G_k=\mu_t\left[2\left(\frac{\partial u}{\partial x}\right)^2+2\left(\frac{\partial v}{\partial y}\right)^2+\left(\frac{\partial u}{\partial y}+\frac{\partial v}{\partial x}\right)^2\right]$$

$$\frac{\mathrm{d}\overline{u_p^{m'^2}}}{\mathrm{d}t} = u_p^m \frac{\mathrm{d}\overline{u_p^{m'^2}}}{\mathrm{d}x} + v_p^m \frac{\mathrm{d}\overline{u_p^{m'^2}}}{\mathrm{d}y} = \frac{2\overline{u_p'^m u'}}{\tau_{rp}^m} - \frac{2\overline{u_p^{m'^2}}}{\tau_{rp}^m} \quad , \tag{7}$$

and

$$\frac{\mathrm{d}\overline{v_p^{m'^2}}}{\mathrm{d}t} = u_p^m \frac{\mathrm{d}\overline{v_p^{m'^2}}}{\mathrm{d}x} + v_p^m \frac{\mathrm{d}\overline{v_p^{m'^2}}}{\mathrm{d}y} = \frac{2\overline{v_p'^m v'}}{\tau_{rp}^m} - \frac{2\overline{v_p^{m'^2}}}{\tau_{rp}^m} \quad , \tag{8}$$

where the turbulent modulation term $\overline{u_p'^m u'}$ and $\overline{v_p'^m v'}$ are proposed by Chen and Wood (1986) as

$$\overline{u_p'^m u'} = \overline{u'^2} \ \exp\left(-B_k \frac{\tau_{rp}^m}{\tau_T}\right) \quad , \tag{9}$$

$$\overline{v_p'^m v'} = \overline{v'^2} \ \exp\left(-B_k \frac{\tau_{rp}^m}{\tau_T}\right) \quad , \tag{10}$$

with the time scale of an energetic eddy τ_T, empirical constants C_T and B_k given as

$$\tau_T = C_T k/\varepsilon \quad , \tag{11}$$

$$C_T = 0.165, \quad B_k = 0.5 \quad . \tag{12}$$

For the stochastic trajectory, the m-th particle's position x_p^m and y_p^m are given as

$$\frac{\mathrm{d}x_p^m}{\mathrm{d}t} = u_p^m + u_p'^m \quad , \tag{13}$$

$$\frac{\mathrm{d}y_p^m}{\mathrm{d}t} = v_p^m + v_p'^m \quad . \tag{14}$$

The time-averaged velocities of the m-th particle u_p^m and v_p^m are determined by Eqs. (2) and (3), respectively. The fluctuating velocities of the m-th particle $u_p'^m$ and $v_p'^m$ are sampled from a Gaussian distribution with zero mean and variances of $\overline{u_p^{m'^2}}$ and $\overline{v_p^{m'^2}}$ obtained from Eqs. (7) and (8) such that

$$u_p'^m = \zeta(\overline{u_p^{m'^2}}) \quad , \tag{15}$$

$$u_p'^m = \zeta(\overline{v_p^{m'^2}}) \quad . \tag{16}$$

After calculating sufficient number of particles, mean properties of the dispersed phase such as velocities u_p, v_p and fluctuating velocities $\overline{u_p'}$, $\overline{v_p'}$ in each control volume are obtained by statistical approach as

$$u_p = \frac{\sum_m n_p^m \Delta\tau_p^m u_p^m}{\sum_m n_p^m \Delta\tau_p^m} \quad , \tag{17}$$

$$v_p = \frac{\sum_m n_p^m \Delta\tau_p^m v_p^m}{\sum_m n_p^m \Delta\tau_p^m} \quad , \tag{18}$$

$$\overline{u_p'^2} = \frac{\sum_m n_p^m \Delta\tau_p^m \overline{u_p^{m'^2}}}{\sum_m n_p^m \Delta\tau_p^m} \quad , \tag{19}$$

$$\overline{v_p'^2} = \frac{\sum_m n_p^m \Delta\tau_p^m \overline{u_p^{m'^2}}}{\sum_m n_p^m \Delta\tau_p^m} \quad , \tag{20}$$

where $\Delta\tau_p^m = t_{\mathrm{out}}^m - t_{\mathrm{in}}^m$ represents the residence time of the m-th computational particle in a control volume. The particle number density n_p is given as

$$n_p = \sum_m \frac{n_p^m \Delta\tau_p^m}{\Delta V} \quad , \tag{21}$$

where ΔV is the control volume. The source terms due to the gas-particle interaction, S_{pu} and S_{pv}, are given by Crowe et al. (1977) as

$$S_{pu} = \sum_m n_p^m \left[\left(\frac{\pi D_p^{m^3}}{6} \rho_p u_p^m \right)_{\mathrm{out}} - \left(\frac{\pi D_p^{m^3}}{6} \rho_p u_p^m \right)_{\mathrm{in}} \right] \Big/ \Delta V \quad , \tag{22}$$

and

$$S_{pv} = \sum_m n_p^m \left[\left(\frac{\pi D_p^{m^3}}{6} \rho_p v_p^m \right)_{\mathrm{out}} - \left(\frac{\pi D_p^{m^3}}{6} \rho_p v_p^m \right)_{\mathrm{in}} \right] \Big/ \Delta V \quad . \tag{23}$$

The time-averaged properties of the dispersed phase including velocity and fluctuating velocity are transported along the stochastic trajectory in the ISSF model. Both effects of the particle's history and its current state on the fluctuation of dispersed phase are included.

Numerical procedure and boundary conditions

In the experiment, a 5.2-m long channel flow development section ensures fully developed flow at the inlet to the test section and allows sufficient time for the particles to come to equilibrium with the channel flow. However, the inlet conditions of the backward-facing step flow are not given in experiment. Therefore, numerical simulation of the 5.2-m long channel flow is first carried out to give the inlet condition of the backward-facing step flow, which includes distribution of velocity, turbulent kinetic energy and its dissipation rate. The distributions of inlet velocity and its fluctuations are shown in Figs. 2–4, where $x/H = 0$. No-slip condition for velocity is used such that u and v are zero at the walls. For k and ε, wall-function approximation for near-wall grid nodes are adopted. At the exit, fully-developed flow conditions are used such that $\partial\varphi/\partial x = 0$ $(\varphi = u, k, \varepsilon)$ and $v = 0$.

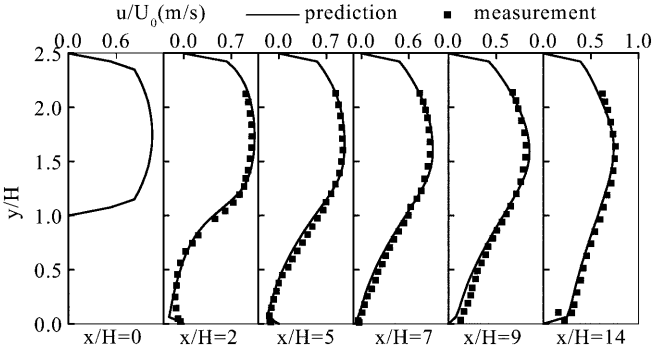

Fig. 2. Streamwise mean velocity

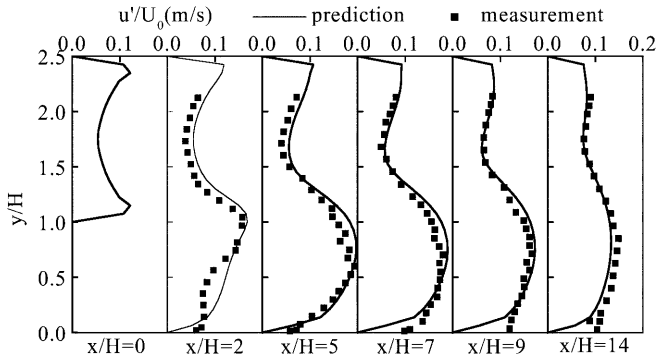

Fig. 3. Streamwise mean fluctuating velocity

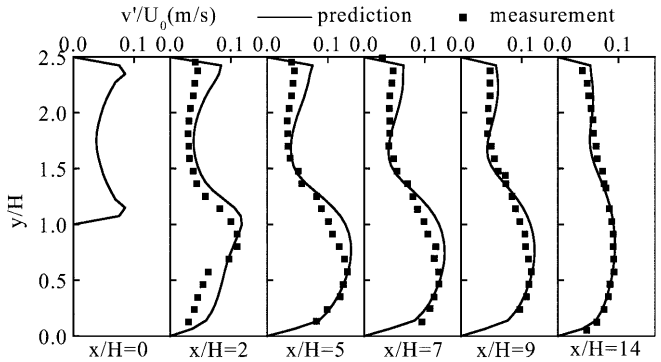

Fig. 4. Transverse mean fluctuating velocity

For the particle phase, streamwise velocities at the inlet correspond to terminal velocities of the experiment which are 0.92 m/s for the 150 μm glass particles and 0.88 m/s for the 70 μm copper particles. Transverse velocities of particles at the inlet are taken to be zero. The streamwise and transverse fluctuating velocities are given as the same as those of the gas phase. It can be seen that the fluctuating status of particle phase at the inlet is easily set using the ISSF model. The elasticity-collision condition is adopted for the particle phase at the walls. Particles are introduced into the flow at 40 different equally spaced inlet positions between $y = 26.7$ and 66.7 mm. In order to verify the sensitivity of the predicted results to the number of calculation particles, 250 and 500 calculation particles are selected for two different simulated cases. For the 250 calculation particles, 15 particles are added into the flow at each of the first five positions near $y = 26.7$ mm and 5 particles at each of other positions. For the 500 calculation particles, 30 particles are added into the flow at each of the first five positions near $y = 26.7$ mm and 10 particles at each of the other positions. The mass flow rate of each particle varies with the inlet position where the particle is added to establish a uniform distribution of particle number density. In order to increase the probability of particle appearing in the recirculating region and improve the predicting results in this region, more particles are added near $y = 26.7$ mm as described above.

The set of partial differential equations of the gas phase are integrated numerically by the SIMPLE algorithm subject to the boundary conditions above. The set of equations of the particle phase are integrated over a time step Δt (of the order 10^{-4} s) by the Eulerian method. In integrating the particle position equations, the action times of each sampled fluctuating velocity of the particle phase are determined. In fact, this action time is related to the energy spectrum and frequency of the particle's fluctuation that are measured by experiments. This prediction is determined by reference to the action time of the gas-phase fluctuating velocity in the SSF model.

The gas-phase flow field is obtained by first solving the governing equations without the source term due to the interaction between the two phases. As the particles move through the above gas-phase flow field the source terms are then introduced. The gas-phase governing equations are solved iteratively with the source terms until convergence is attained. The convergence criterion is that the sum of the absolute values of the momentum residual is less than 10^{-6}.

Results and discussion

Predicted and measured results of the streamwise velocities as well as streamwise and transverse fluctuating velocities of the gas phase are shown in Figs. 2–4, respectively. As fluctuating velocities cannot be obtained directly using the k–ε turbulence model, the ratio of streamwise mean-square fluctuating velocity $\overline{u'^2}$ to transverse mean-square fluctuating velocity $\overline{v'^2}$ is assumed as 2:1 in predictions for the gas phase. It can be seen that the predicted mean velocities and fluctuating velocities are in good agreement with Fessler's experiment. It indicates that the backward-facing step flow is anisotropic and the assumed ratio is correct. As is well known, the reattachment length predicted using k–ε model is much less than that of experiment. However, in our predictions, the predicted reattachment length is $7.4H$ as shown in Fig. 5, which agrees well with the experimental value of $7.6H$. This is mainly due to the accurate inlet conditions and adjustment of model constants as shown in Table 2.

Predicted and measured results of the streamwise velocities as well as streamwise and transverse fluctuating velocities of 150 μm glass and 70 μm copper particle phase are shown in Figs. 6–11, respectively. These show that the predicted mean velocities and fluctuating velocities agree well with those of the experiment. The characteristic difference between the streamwise mean fluctuating velocity and transverse mean fluctuating velocity can be seen from predicted results and experiment values. This indicates

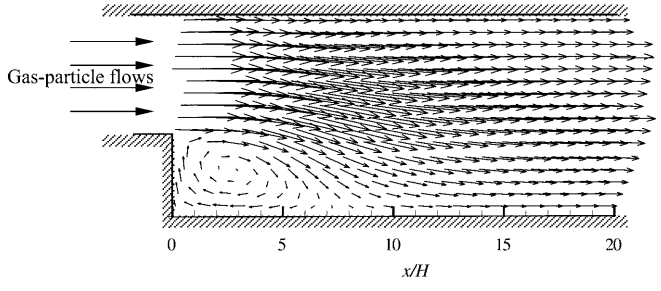

Fig. 5. Flow pattern

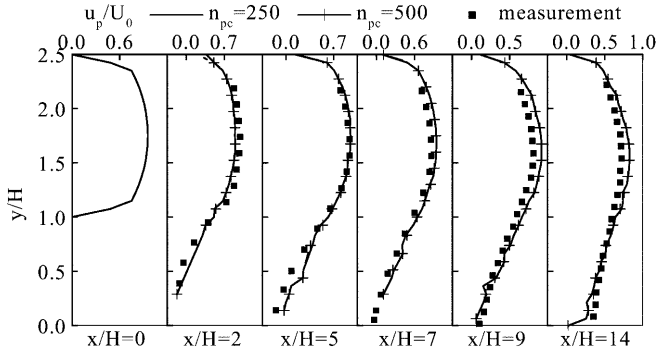

Fig. 6. Streamwise mean velocity for glass particles

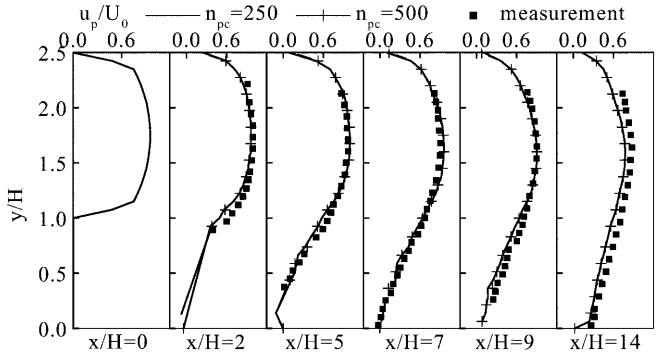

Fig. 9. Streamwise mean velocity for copper particles

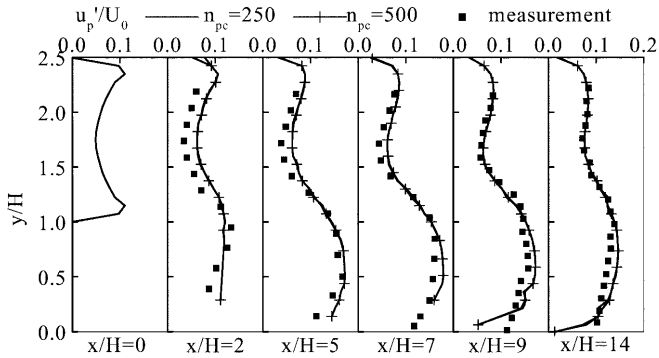

Fig. 7. Streamwise mean fluctuating velocity for glass particles

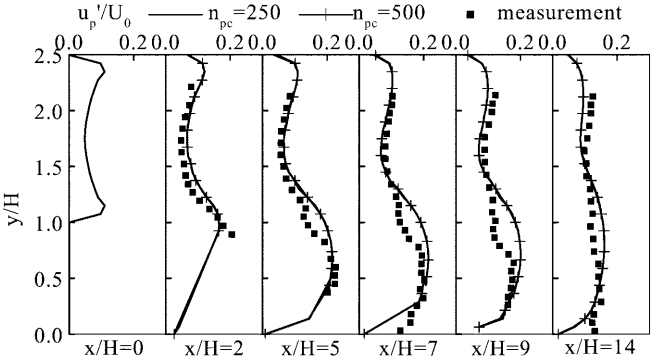

Fig. 10. Streamwise mean fluctuating velocity for copper particles

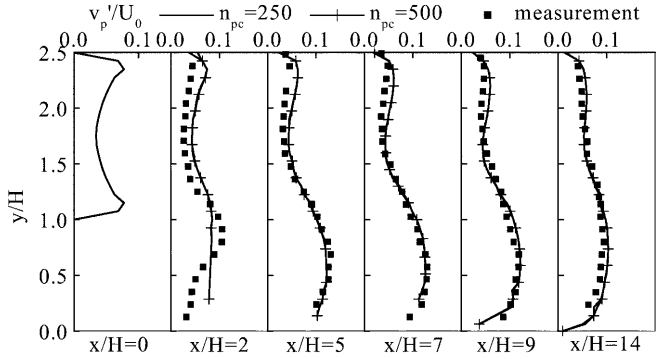

Fig. 8. Transverse mean fluctuating velocity for glass particles

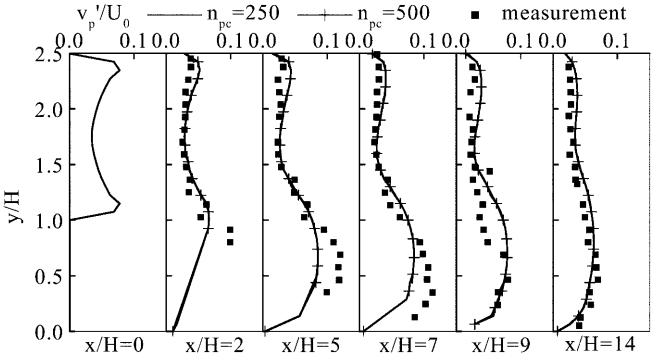

Fig. 11. Transverse mean fluctuating velocity for copper particles

that the ISSF model has a good ability for predicting anisotropic turbulent particle flows. For inlet conditions of the fluctuating velocity of the particle phase, it is easily considered using the ISSF model by taking corresponding inlet conditions as initial conditions of Eqs. (7) and (8). 150 μm glass particles can be found in the recirculating regions in the prediction and in the experiment, while 70 μm copper particles are not found in the recirculating region in the experiment. Sensitivity of the predicted results to the number of calculation particles is also studied. As shown in Figs. 6–11, there is no significant difference in the predicted results of particle phase for using 250 and 500 particles. For similar cases using the conventional SSF model, 10,000 particles were used for computing the mono-dispersed particle laden jet by Mostafa et al. (1989) and 9000 computation particles were needed for smooth profiles of predictions in a confined particle-laden jet by Adeniji-Fashola and Chen (1990). Unlike the conventional stochastic separated flow model which requires many more computation particles, the present study using the ISSF model requires far less particles (<250) in obtaining smooth statistical and reasonable results.

The distributions of particle number density are shown in Fig. 12. The distribution becomes uniform from upstream to downstream, which is very similar to the experiment. Chang and Yang (1999) reviewed some numerical issues of the stochastic Eulerian-Lagrangian models for two-phase turbulent flow computations. They concluded that inlet condition of the dispersed-phase fluctuating velocity has an important effect on predicted

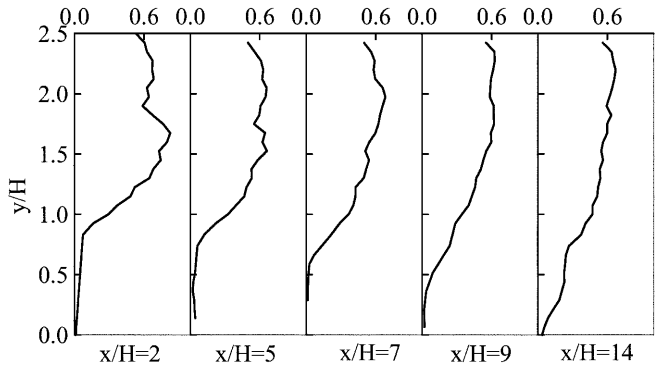

Fig. 12. Dimensionless particle number density

results of the fluctuating flow quantity of the dispersed phase. Such inlet condition is generally neglected in other stochastic Lagrangian computations. In addition, a large number of computational particles (in excess of 10^4) for each size is needed to attain a statistically stationary solution of $\overline{u_p'^2}$ and $\overline{v_p'^2}$. These issues are successfully resolved in numerical simulation of backward-facing step gas-particle flows using the ISSF model.

In the ISSF model, the inlet condition of the dispersed-phase fluctuating velocity is easily introduced into the computations without increasing any of the stochastic trajectory. The solved quantities of the dispersed phase along the stochastic trajectory are time-averaged velocity and root-mean-square of fluctuating velocity. In this respect, in the ISSF model, the interaction between the two phases are considered to be a continuous process, which is similar to the DSF model and different from the SSF model. This is the key factor why the ISSF model requires far less computation particles to obtain a statistically stationary solution of mean velocity and root-mean-square fluctuating velocity. Therefore, compared with SSF model, the ISSF model has the advantage of easy manipulation of inlet conditions of the dispersed phase and far less computational particles to obtain statistically smooth solutions.

Conclusions

Using the ISSF model, predicted results of velocity and fluctuating velocity of both phases of backward-facing step flow are in good agreement with the experiment. Distributions of particle number density are very similar to that of the experiment. As the inlet condition is easily introduced into the computations and the quantities solved along the trajectory are not related to the instantaneous quantities, the ISSF model requires fewer particles in obtaining smooth and reasonable statistical results. It is concluded that the ISSF model is successfully applied in predicting backward-facing step flow.

References

Adeniji-Fashola, Chen CP (1990) Modeling of confined turbulent fluid-particle flows using Eulerian and Lagrangian schemes. Int. J. Heat Mass Transfer 33: 691–701

Chan CK, Zhang HQ, Lau KS (2000) An improved stochastic separated flow model for turbulent two-phase flow. Comput. Mech. 24: 491–502

Chang KC, Wu WJ (1994) Sensitivity study on Monte Carlo solution procedure of two-phase turbulent flow. Numer. Heat Transfer, Part B 25: 223–244

Chang KC, Yang JC (1999) Revisiting numerical issues of stochastic Eulerian–Lagrangian models. Proceedings of the third ASME/JSME Joint Fluids Engineering Conference, San Francisco, California, USA

Chen CP, Wood PE (1986) Turbulence closure modeling of the dilute gas-particle asymmetric jet. AIChE J. 32: 163–166

Crowe CT, Sharma MP, Stock DE (1977) The particle source-in-cell methods for gas-droplet flows. J. Fluid Eng. 99: 325–332

Crowe CT, Troutt TR, Chung JN (1996) Numerical models for two-phase turbulent flows. Ann. Rev. Fluid Mech. 28: 11–43

Fessler JR, Eaton JK (1999) Turbulent modification by particle in a backward-facing step flow. J. Fluid Mech. 394: 97–117

Mostafa AA, Mongia HC, McDonell VG, Samuelsen GS (1989) Evolution of particle-laden jet flows: a theoretical and experimental study. AIAA J. 27: 167–183

Putnam A (1961) Integrable form of droplet drag coefficient. ARSJ 31: 1467–1468

Zhang HQ, Chan CK, Lau KS (2001) Numerical simulation of sudden-expansion particle-laden flows using an improved stochastic separated flow model. Numer. Heat Transfer, Part B in press